Biomolecular Feedback Systems

Domitilla Del Vecchio
U. Michigan/MIT

Richard M. Murray
Caltech

DRAFT v0.3, March 30, 2010

Chapter 6
Biological Circuit Components

6.1 Biological Circuit Design

One of the fundamental building blocks employed in synthetic biology is the process of transcriptional regulation, which is found in natural transcriptional networks. A transcriptional network is composed of a number of genes that express proteins that then act as transcription factors for other genes. The rate at which a gene is transcribed is controlled by the *promoter*, a regulatory region of DNA that precedes the gene. RNA polymerase binds a defined site (a specific DNA sequence) on the promoter. The quality of this site specifies the transcription rate of the gene (the sequence of the site determines the chemical affinity of RNA polymerase to the site). RNA polymerase acts on all of the genes. However, each transcription factor modulates the transcription rate of a set of target genes. Transcription factors affect the transcription rate by binding specific sites on the promoter region of the regulated genes. When bound, they change the probability per unit time that RNA polymerase binds the promoter region. Transcription factors thus affect the rate at which RNA polymerase initiates transcription. A transcription factor can act as a *repressor* when it prevents RNA polymerase from binding to the promoter site. A transcription factor acts as an *activator* if it facilitates the binding of RNA polymerase to the promoter. Such interactions can be generally represented as nodes connected by directed edges. Synthetic bio-molecular circuits are fabricated typically in bacteria *E. coli*, by cutting and pasting together according to a desired sequence genes and promoter sites (natural and engineered). Since the expression of a gene is under the control of the upstream promoter region, one can this way create a desired circuit of activation and repression interactions among genes. Early examples of such circuits include an activator-repressor system that can display toggle switch or clock behavior [6], a loop oscillator called the repressilator obtained by connecting three inverters in a ring topology [18], a toggle switch obtained connecting two inverters in a ring fashion [20], and an autorepressed circuit [10] (Figure 6.1). Several scientific and technological developments accumulating over the past four decades have set the stage for the design and fabrication of early synthetic bio-molecular circuits (Figure 6.2).

An early milestone in the history of synthetic biology can be traced back to the discovery of mathematical logic in gene regulation. In their 1961 paper, Jacob and Monod introduced for the first time the idea of gene expression regulation through transcriptional feedback [31]. Only a few years later (1969), special enzymes that

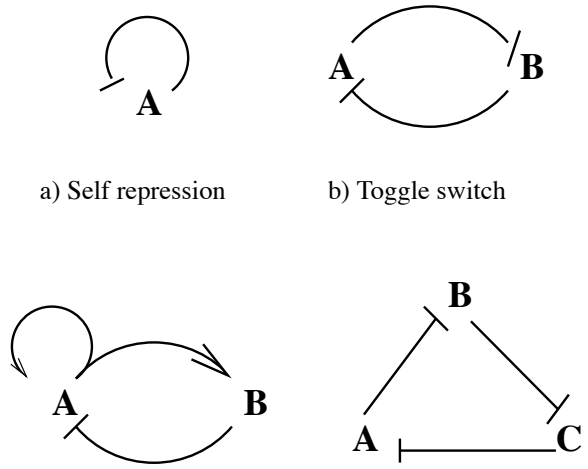

a) Self repression b) Toggle switch

c) Activator-repressor clock d) Repressilator

Figure 6.1: Early transcriptional circuits that have been fabricated in bacteria *E. coli*: the self-repression circuit [10], the toggle switch [20], the activator-repressor clock [6], and the repressilator [18]. Each node represents a gene and each arrow from node Z to node X indicates that the transcription factor encoded in z, denoted Z, regulates gene x [3]. If z represses the expression of x, the interaction is represented by Z⊣X. If z activates the expression of x, the interaction is represented by Z→X [3].

can cut double-stranded DNA at specific recognition sites (known as restriction sites) were discovered by Arber and co-workers [4]. These enzymes, called restriction enzymes, were major enabler of recombinant DNA technology. One of the most celebrated products of such a technology is the large scale production of insulin by employing *E. coli* bacteria as a cell factory [57]. The development of recombinant DNA technology along with the demonstration in 1970 that genes can be artificially synthesized, provided the ability to cut and paste natural or synthetic promoters and genes in almost any fashion on size-wise compatible plasmids. This "cut and paste" procedure is called *cloning* [2]. Cloning of any DNA fragment involves four steps: *fragmentation, ligation, transfection*. The DNA of interest is first isolated. Then, a ligation procedure is employed in which the amplified fragment is inserted into a vector. The vector (which is frequently circular) is linearized by means of restriction enzymes that cleave it at target sites called restriction sites. It is then incubated with the fragment of interest with an enzyme called *DNA ligase*. Polymerase chain reaction (PCR), devised in the 1980s, allows then to exponentially amplify a small amount of DNA in amounts large enough to be used for transfection and transformation in living cells [2]. Today, commercial synthesis of DNA sequences and genes has become cheaper and faster with a price often below $ 1 per base pair [8].

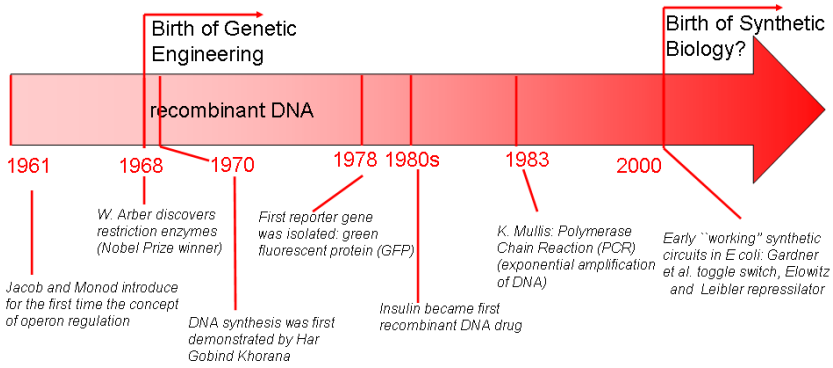

Figure 6.2: Milestones in the history of synthetic biology.

In this part, we analyze the behavior of the early modules fabricated so far by employing several of the techniques that we have studied in the previous chapters.

6.2 Self-repressed gene

In this section, we analyze the self repressed gene of Figure 6.1 and focus on analyzing how the presence of the negative feedback affects the dynamics of the system [46] and how the negative feedback affects the noise properties of the system [10, 7].

Let X denote the concentration of protein X and let X be a transcriptional repressor for its own production. Assuming that the mRNA dynamics are at the quasi steady state, the ODE model describing the self repressed system is given by

$$\dot{X} = \frac{\beta}{1 + X/K} - \delta X,$$

in which we have assumed that the Hill coefficient is equal to 1. We seek to compare the behavior of this autoregulated system to the behavior of the unregulated one:

$$\dot{X} = \beta_0 - \delta X,$$

in which β_0 is the unrepressed production rate.

Dynamic effects of negative feedback

We show here that the rise time of the system decreases due to the presence of the negative feedback, that is, the dynamics become faster. For the unrepressed system, we obtain (by direct integration) the behavior of $X(t)$ as

$$X(t) = \frac{\beta_0}{\delta}(1 - e^{-\delta t}),$$

in which we have assumed zero initial condition. For the self repressed system, assuming that $X(t)$ is sufficiently small, we can use Taylor expansion about $X = 0$ to approximate the dynamics about $X = 0$ by $\dot{X} = \beta - \bar{\delta}X + O(X^2)$, in which $\bar{\delta} = -\delta - \frac{\beta}{K}$. As a consequence, we have that

$$X(t) = \frac{\beta}{\bar{\delta}}(1 - e^{-\bar{\delta}t}).$$

The rise time is the time $X(t)$ takes to go from 10% of its final value to 90% of its final value. In this case, we thus have that for the unrepressed system the rise time is $2/\delta$, while for the self-repressed system is given by $2/\bar{\delta}$. Since $\bar{\delta} > \delta$, we have that the rise time for the self-repressed system is smaller and hence its dynamics are faster. This was experimentally confirmed by [46].

Noise filtering

In this section, we investigate the effect of the negative feedback on the noise spectrum of the system. Specifically, we employ the Langevin modeling framework to show that the presence of a negative feedback decreases the amplitude of the noise at low frequency, while it increases it at higher frequency. In order to show this fact, we perform here a simplified analysis, in which we model the unrepressed system by the reactions

$$\phi \xrightarrow{\beta_0} \mathrm{X}, \quad \mathrm{X} \xrightarrow{\delta} \phi$$

and the self repressed system, following the approximations of the previous section, by the reactions

$$\phi \xrightarrow{\beta} \mathrm{X}, \quad \mathrm{X} \xrightarrow{\bar{\delta}} \phi$$

in which $\bar{\delta} = -\delta - \frac{\beta}{K}$. The reader can as an exercise model the self-repressed system by considering all the involved reactions including the binding of the repressor to DNA and verify that a result similar to the one we are about to show here follows.

As we have seen previously, the concentration $X(t)$ in a stochastic model is a random variable. In the Langevin approximation, it is given by $X(t) = \phi(t) + \frac{1}{\sqrt{\Omega}}Z(t)$, in which $\phi(t)$ is the solution to the deterministic system while $Z(t)$ is a zero-mean random variable whose dynamics is determined by the Langevin equation:

$$\dot{Z}(t) = AZ(t) + B\Gamma(t),$$

in which $A = \frac{\partial S f(X)}{\partial X}|_{X=\phi(t)}$ with S the stoichiometry matrix and $f(X)$ is the vector of reactions, while $B = S\sqrt{\mathrm{diag}(f(\phi(t))}$. The vector $\Gamma(t)$ has entries given by realizations of white noise, in which each entry i models the noise on the *ith* reaction. In the case in consideration, we are interested in the spectrum of the noise on the steady state value of the system, so that $\phi(t) = X_0$ with X_0 the steady state value. Here, we assume for simplicity that the steady state value of the same for both the

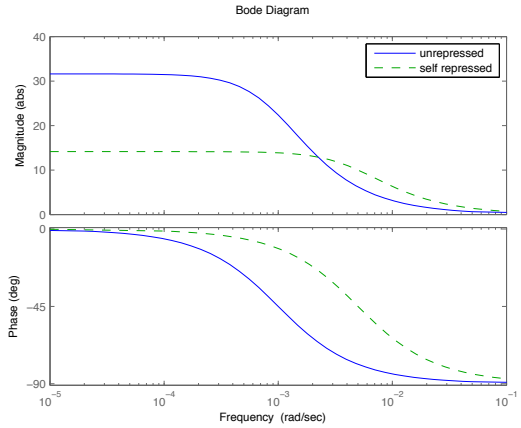

Figure 6.3: Bode plots of the transfer function $T_{\Gamma_2 \to Z}(s)$ for both unrepressed (solid) and self repressed (dashed) systems.

self repressed and the unrepressed system. For the unrepressed system, we have that

$$f(X) = [\beta_0 \ \delta X]', \ S = [1 \ -1], \ A = -\delta, \ B = [1 \ -1] \begin{bmatrix} \sqrt{\beta_0} & 0 \\ 0 & \sqrt{\delta X_0} \end{bmatrix} = [\sqrt{\beta_0} \ -\sqrt{\delta X_0}],$$

while for the self repressed system we have that

$$f(X) = [\beta \ \bar{\delta} X]', \ S = [1 \ -1], \ A = -\bar{\delta}, \ B = [1 \ -1] \begin{bmatrix} \sqrt{\beta} & 0 \\ 0 & \sqrt{\bar{\delta} X_0} \end{bmatrix} = [\sqrt{\beta} \ -\sqrt{\bar{\delta} X_0}].$$

It follows that the Langevin equations are given by

$$\dot{Z}(t) = -\delta Z(t) + \sqrt{\beta_0}\Gamma_1 - \sqrt{\delta X_0}\Gamma_2$$

for the unrepressed system and by

$$\dot{Z}(t) = -\bar{\delta} Z(t) + \sqrt{\beta}\Gamma_1 - \sqrt{\bar{\delta} X_0}\Gamma_2$$

for the self repressed system.

We can calculate the noise spectrum by simply calculating the transfer function from Γ_i to Z, that is, $T_{\Gamma_i \to Z}(s)$ and by computing their amplitudes $A_{\Gamma_i \to Z}(\omega) = \sqrt{T_{\Gamma_i \to Z}(j\omega)}$. This gives the expressions

$$A_{\Gamma_1 \to Z}(\omega) = \frac{\sqrt{\beta_0}}{\sqrt{\omega^2 + \delta^2}}, \ A_{\Gamma_2 \to Z}(\omega) = \frac{\sqrt{\delta X_0}}{\sqrt{\omega^2 + \delta^2}}$$

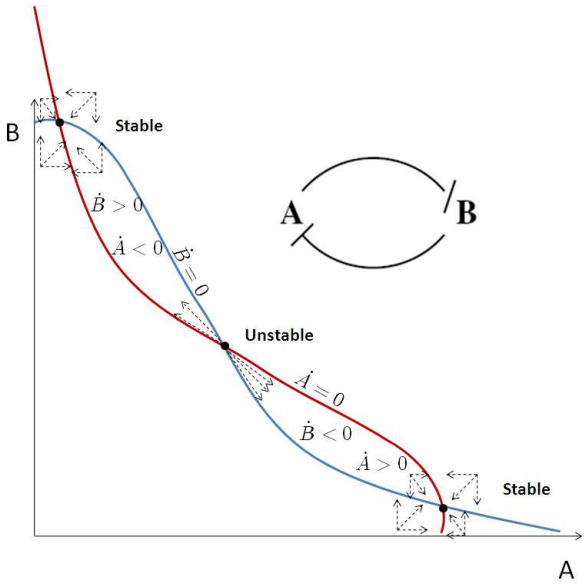

Figure 6.4: Nullclines for the toggle switch. By analyzing the direction of the vector field in the proximity of the equilibria, one can deduce their stability.

for the unrepressed system and

$$A_{\Gamma_1 \to Z}(\omega) = \frac{\sqrt{\beta}}{\sqrt{\omega^2 + \bar{\delta}^2}}, \quad A_{\Gamma_2 \to Z}(\omega) = \frac{\sqrt{\bar{\delta} X_0}}{\sqrt{\omega^2 + \bar{\delta}^2}}$$

for the self repressed system. Figure 6.3 shows the amplitude $A_{\Gamma_i \to Z}(\omega) = \sqrt{T_{\Gamma_2 \to Z}(j\omega)}$. Since $\bar{\delta} > \delta$, we have that the amplitude of the noise on X at low frequency is lower for the self repressed circuit, while at higher frequency it is higher for the self repressed circuit. This illustrates the spectral shift of the intrinsic noise toward the high frequency as also experimentally demonstrated by [7].

6.3 The Toggle Switch

The toggle switch is composed of two genes that mutually repress each other as shown in the diagram of Figure 6.4 [20]. By assuming that the mRNA dynamics are at the quasi steady state, we obtain two dimensional ODE model given by

$$\begin{aligned} \dot{A} &= \frac{\beta}{1 + (B/K)^n} - \delta A \\ \dot{B} &= \frac{\beta}{1 + (A/K)^n} - \delta B, \end{aligned}$$

in which we have assumed for simplifying the analysis that the parameters of the repression functions are the same for A and B. The number and stability of equilibria can be analyzed by performing nullcline analysis since the system is two-dimensional. Specifically, by setting $\dot{A} = 0$ and $\dot{B} = 0$, we obtain the nullclines shown in Figure 6.4. In the case in which the parameters are the same for both A and B, the nullcline always intersect in three points, which determine the steady states of this system. The nullclines partition the plane into six regions. By determining the sign of $\dot{A}$ and $\dot{B}$ in each of these six regions, one determines the direction in which the vector field is pointing in each of these regions (see Figure 6.4). From these directions, one immediately deduces that the steady state for which $A = B$ is instable while the other two are stable. This is thus a bistable system. When the system converges to one steady steady or the other depending on whether the initial condition is in the region of attraction of one steady state or the other. Once the system has converged to one of the two steady states, it cannot switch to the other unless an external stimulation is applied that moves the initial condition to the region of attraction of the other steady state [20]. Note that a bistable system, when subject to noise, can give rise to noise-induced oscillations.

6.4 The repressilator

Elowitz and Leibler [18] constructed the first operational oscillatory genetic circuit consisting of three repressors arranged in ring fashion, and coined it the "repressilator" (See diagram d) of Figure 6.1). The repressilator exhibits sinusoidal, limit cycle oscillations in periods of hours. The dynamical model of the repressilator can be obtained by composing three transcriptional modules in a loop fashion. The dynamics can be written as

$$\begin{aligned} \dot{r}_A &= -\delta r_A + f_1(C) \\ \dot{A} &= r_A - \delta A \\ \dot{r}_B &= -\delta r_B + f_2(A) \\ \dot{B} &= r_B - \delta B \\ \dot{r}_C &= -\delta r_C + f_3(B) \\ \dot{C} &= r_C - \delta C, \end{aligned} \tag{6.1}$$

in which in the original design[18], we had that

$$f_1(p) = f_2(p) = f_3(p) = \frac{\alpha^2}{1 + p^n}.$$

This structure belongs to the class of cyclic feedback systems that we have studied in earlier chapters. In particular, Mallet-Paret and Smith Theorem [37] and Hastings Theorem [27] (see Chapter 3 for the details) can be applied to infer that if the

system has a unique equilibrium point and this is unstable, then it admits a periodic solution. Therefore, we first determine the number of equilibria and then their stability. The equilibria of the system can be found by setting the time derivatives to zero. We thus obtain that

$$A = \frac{f_1(C)}{\delta^2}, \;\; B = \frac{f_2(A)}{\delta^2}, \;\; C = \frac{f_3(B)}{\delta^2},$$

which combined together yield to

$$A = \frac{1}{\delta^2} f_1\left(\frac{1}{\delta^2} f_3\left(\frac{1}{\delta^2} f_2(A)\right)\right) =: g(A).$$

The solution to this equation determines the set of steady states of the system. The system will have one steady state if $g'(A) = \frac{dg(A)}{dA} < 0$, otherwise, it could have multiple steady states. Since we have that

$$\text{sign}(g'(A)) = \Pi_{i=1}^3 \text{sign}(f_i'(P)),$$

then if $\Pi_{i=1}^3 \text{sign}(f_i'(P)) < 0$ the system has a unique steady state. We name the product $\Pi_{i=1}^3 \text{sign}(f_i'(P))$ *loop gain*. Thus, any cyclic feedback system with negative loop gain will have a unique steady state. It can be shown that a cyclic feedback system with positive loop gain belongs to the class of monotone system and hence cannot have periodic orbits [37]. In the present case, system 6.1 is such that $f_i' < 0$, so that the loop gain is negative and there is a unique steady state. We next study the stability of this steady state by studying the Jacobian of the system.

Denoting by P the steady state value of the protein concentrations for A, B, and C, the Jacobian of the system is given by

$$J = \begin{bmatrix} -\delta & 0 & 0 & 0 & 0 & f_1'(P) \\ 1 & -\delta & 0 & 0 & 0 & 0 \\ 0 & f_2'(P) & -\delta & 0 & 0 & 0 \\ 0 & 0 & 1 & -\delta & 0 & 0 \\ 0 & 0 & 0 & f_3'(P) & -\delta & 0 \\ 0 & 0 & 0 & 0 & 1 & -\delta \end{bmatrix},$$

whose characteristic polynomial is given by $p(\lambda) = \det(\lambda I - J) = (\lambda+\delta)^6 - \Pi_{i=1}^3 f_i'(P)$. In the case in which $f_i(P) = \frac{\alpha^2}{1+P^n}$ for $i \in \{1,2,3\}$, this characteristic polynomial has a root with positive real part if the ratio α/δ satisfies the relation

$$\alpha^2/\delta^2 > \sqrt[n]{\frac{4/3}{n-4/3}}(1 + \frac{4/3}{n-4/3}).$$

For the proof of this statement, the reader is referred to [16]. This relationship is plotted in the left plot of Figure 6.5. When n increases, the existence of an unsta-

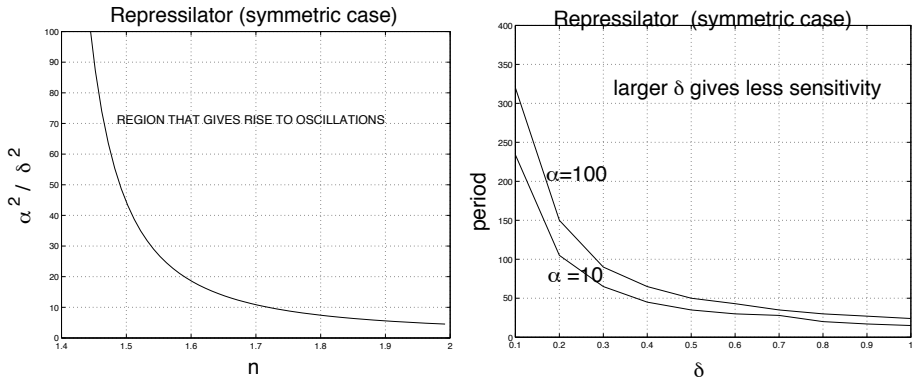

Figure 6.5: (Left) Space of parameters that give rise to oscillations for the repressilator in equations (6.1). (Right) Period as a function of δ and α.

ble equilibrium point is guaranteed for larger ranges of the other parameter values. Equivalently, for fixed values of α and δ, as n increases the robustness of the circuit oscillatory behavior to parametric variations in the values of α and δ increases. Of course, this "behavioral" robustness does not guarantee that other important features of the oscillator, such as the period value, are slightly changed when parameters vary. Numerical studies indicated that the period T approximatively follows $T \propto \frac{1}{\delta}$, and varies only little with α (right plot of Figure 6.5). From the figure, we can note that as the value of δ increases, the sensitivity of the period to the variation of δ itself decreases. However, increasing δ would necessitate the increase of the cooperativity n, therefore indicating a possible trade off that should be taken into account in the design process in order to balance the system complexity and robustness of the oscillations.

A similar result for the existence of a periodic solution can be obtained for the non-symmetric case in which the input functions of the three transcriptional modules are modified to

$$\begin{aligned} f_1(p) &= \frac{\alpha_3^2}{1+p^n} \\ f_2(p) &= \frac{\alpha^2 p^n}{1+p^n} \\ f_3(p) &= \frac{\alpha^2 p^n}{1+p^n}, \end{aligned}$$

that is, two interactions are activations and one only is a repression. Since the loop gain is still negative, there is one equilibrium point only. We can thus obtain the condition for oscillations again by establishing conditions on the parameters that guarantee that at least one root of the characteristic polynomial **??** has positive

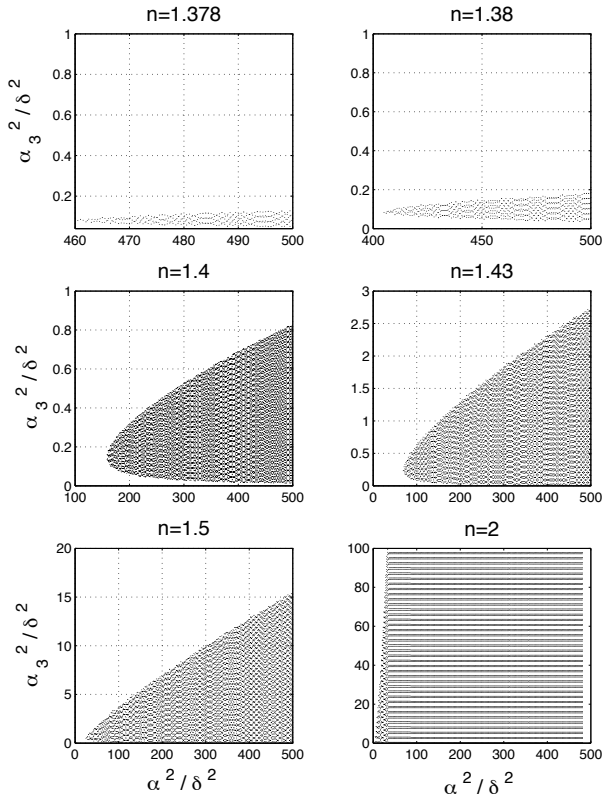

Figure 6.6: Space of parameters that give rise to oscillations for the repressilator (non-symmetric case).

real part. These conditions are reported in Figure 6.6 (see [16] for the detailed derivations). One can conclude that it is possible to "over design" the circuit to be in the region of parameter space that gives rise to oscillations. It is also possible to show that increasing the number of elements in the oscillatory loop, the value of n sufficient for oscillatory behavior decreases. The design criteria for obtaining oscillatory behavior are thus summarized in Figures 6.5 and 6.6.

6.5 Activator-repressor clock

Consider the activator-repressor clock diagram shown in Figure 6.1 c). The transcriptional module for A has an input function that takes two inputs: an activator A and a repressor B. The transcriptional module B has an input function that takes only an activator A as its input. Let r_A and r_B represent the concentration of m-RNA of the activator and of the repressor, respectively. Let A and B denote the protein

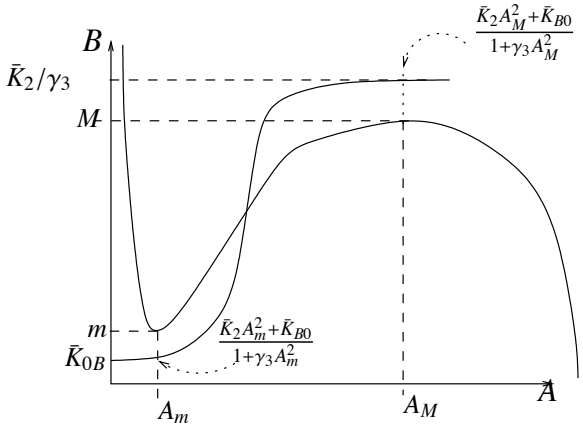

Figure 6.7: Shape of the curves in the A, B plane corresponding to $\dot{r}_B = 0, \dot{B} = 0$ and to $\dot{r}_A = 0, \dot{A} = 0$ as function of the parameters. Letting, $\bar{K}_1 = K_1(k_1/(\delta_1\delta_A))$, $\bar{K}_{A0} = K_{A0}(k_1/(\delta_1\delta_A))$, $\bar{K}_2 = K_2(k_2/(\delta_2\delta_B))$, $\bar{K}_{B0} = K_{B0}(k_2/(\delta_2\delta_B))$, we have $A_m = \frac{\bar{K}_1}{6\gamma_1}\left(1-(cos(\phi/3)-\sqrt{3}sin(\phi/3))\right)$, $A_M = \frac{\bar{K}_1}{6\gamma_1}+\frac{\bar{K}_1}{3\gamma_1}cos(\phi/3)$, $\phi = \text{atan}\left(\frac{\sqrt{\frac{27\bar{K}_{A0}}{4\gamma_1^2}(\frac{\bar{K}_1^3}{\gamma_1^2}-27\bar{K}_{A0})}}{\frac{\bar{K}_1^3}{4\gamma_1^3}-27\frac{\bar{K}_{A0}}{2\gamma_1}}\right)$, $m = \sqrt{\frac{\bar{K}_1 A_m^2+\bar{K}_{A0}-A_m(1+\gamma_1 A_m^2)}{\gamma_2 A_m}}$, $M = \sqrt{\frac{\bar{K}_1 A_M^2+\bar{K}_{A0}-A_M(1+\gamma_1 A_M^2)}{\gamma_2 A_M}}$.

concentration of the activator and of the repressor, respectively. Then, we consider the following four-dimensional model describing the rate of change of the species concentrations:

$$\begin{aligned}
\dot{r}_A &= -\delta_1 r_A + F_1(A,B) \\
\dot{A} &= -\delta_A A + k_1 r_A \\
\dot{r}_B &= -\delta_2 r_B + F_2(A) \\
\dot{B} &= -\delta_B B + k_2 r_B,
\end{aligned} \tag{6.2}$$

in which the functions F_1 and F_2 are the input functions and are given by

$$\begin{aligned}
F_1(A,B) &= \frac{K_1 A^n + K_{A0}}{1+\gamma_1 A^n + \gamma_2 B^n} \\
F_2(A) &= \frac{K_2 A^n + K_{B0}}{1+\gamma_3 A^n}.
\end{aligned}$$

Two-dimensional analysis. We first assume the mRNA dynamics to be at the QSS and perform a two dimensional analysis to invoke Poincarè-Bendixson Theorem. Then, we analyze the four dimensional system and perform a bifurcation study. We thus denote $f_1(A,B) := \frac{k_1}{\delta_1}F_1(A,B)$ and $f_2(A) := \frac{k_2}{\delta_2}F_2(A)$ and $\bar{K}_1 := K_1\frac{k_1}{\delta_1}$,

$\bar{K}_{A0} := K_{A0}\frac{k_1}{\delta_1}$, $\bar{K}_2 := K_2\frac{k_2}{\delta_2}$, and $\bar{K}_{B0} := K_{B0}\frac{k_2}{\delta_2}$. For simplicity, we also denote $f(A,B) := -\delta_A + f_1(A,B)$ and $g(A,B) := -\delta_B B + f_2(A)$ so that the two-dimensional system is given by

$$\begin{aligned} \dot{A} &= f(A,B) \\ \dot{B} &= g(A,B). \end{aligned}$$

For simplicity, we assume $m = 1$ and $\gamma_i = 1$ for all i. We then study whether the system admits a periodic solution for $n = 1$. We analyze the nullclines to determine the number and location of steady states. Specifically, $g(A,B) = 0$ leads to $B = \frac{\bar{K}_2 A + \bar{K}_{B0}}{(1+A)\delta_A}$, which is an increasing function of A. Setting $f(A,B) = 0$, we obtain that $B = \frac{\bar{K}_1 A + \bar{K}_{A0} - \delta_A A(1+A)}{\delta_A A}$, which is a monotonically increasing function of A. As a consequence, we have one equilibrium only. The Jacobian of the system at this equilibrium is given by

$$J = \begin{bmatrix} \frac{\partial f}{\partial A} & \frac{\partial f}{\partial B} \\ \frac{\partial g}{\partial A} & \frac{\partial g}{\partial B} \end{bmatrix}.$$

In order for the equilibrium to be unstable and not a saddle, it is necessary and sufficient that

$$\text{Trace}(J) > 0 \text{ and } \det(J) > 0,$$

in which $\text{Trace}(J) = \frac{\partial f}{\partial A} + \frac{\partial g}{\partial B}$. Since at the equilibrium point we have that

$$\frac{dB}{dA}|_{f(A,B)=0} < 0$$

and by the implicit function theorem $\frac{dB}{dA}|_{f(A,B)=0} = -\frac{\partial f/\partial A}{\partial f/\partial B}$, we have that $\frac{\partial f}{\partial A} < 0$ because $\frac{\partial g}{\partial B} < 0$. As a consequence, we have that $\text{Trace}(J) < 0$ and hence the equilibrium point it either stable or a saddle. Furthermore, the nullclines are such that

$$\frac{dB}{dA}|_{g(A,B)=0} > \frac{dB}{dA}|_{f(A,B)=0},$$

and since by the implicit function theorem we also have that $\frac{dB}{dA}|_{g(A,B)=0} = -\frac{\partial g/\partial A}{\partial g/\partial B}$, it follows that $\det(J) > 0$. Hence, the steady state is always stable and therefore, the omega-limit set of any point on the plane cannot be a periodic orbit.

We now assume that $n = 2$. In this case, the nullcline $f(A,B) = 0$ leads to the set depicted in Figure 6.7 for suitable relationships among the values of the $\bar{K}$'s. In order for the equilibrium to be unstable and not a saddle, we require that $\text{Trace}(J) > 0$, which leads to

$$\frac{\delta_B}{\partial f_1/\partial A - \delta_A} < 1.$$

Further, one can verify that the crossing of the nullclines given in Figure 6.7 leads to $\det(J) > 0$ just as in the case $n = 1$.

Four-dimensional analysis. Then, we consider the following four-dimensional model describing the rate of change of the species concentrations:

$$\begin{aligned} \dot{r}_A &= -\delta_1/\epsilon\, r_A + F_1(A,B) \\ \dot{A} &= \nu(-\delta_A A + k_1/\epsilon\, r_A) \\ \dot{r}_B &= -\delta_2/\epsilon\, r_B + F_2(A) \\ \dot{B} &= -\delta_B B + k_2/\epsilon\, r_B, \end{aligned} \tag{6.3}$$

in which the parameter ν regulates the difference of time-scales between the repressor and the activator dynamics, ϵ is a parameter that regulates the difference of time-scales between the m-RNA and the protein dynamics. The parameter ϵ determines how close model (6.3) is to a two-dimensional model in which the m-RNA dynamics are considered at the equilibrium. Thus, ϵ is a singular perturbation parameter (equations (6.3) can be taken to standard singular perturbation form by considering the change of variables $\bar{r}_A = r_A/\epsilon$ and $\bar{r}_B = r_B/\epsilon$). The details on singular perturbation can be found in Chapter 3. The values of ϵ and of ν do not affect the number of equilibria of the system, while the values of the other parameters are the ones that control the number of equilibria. The set of values of $K_i, k_i, \delta_i, \gamma_i, \delta_A, \delta_B$ that allow the existence of a unique equilibrium can be determined by employing graphical techniques. In particular, we can plot the curves corresponding to the sets of A, B values for which $\dot{r}_B = 0$ and $\dot{B} = 0$ and the set of A, B values for which $\dot{r}_A = 0$ and $\dot{A} = 0$ as in Figure 6.7. The intersection of these two curves provides the equilibria of the system and conditions on the parameters can be determined that guarantee the existence of one equilibrium only. In particular, we require that the basal activator transcription rate when B is not present, which is proportional to $\bar{K}_{A0}$, is sufficiently smaller than the maximal transcription rate of the activator, which is proportional to $\bar{K}_1$. Also, $\bar{K}_{A0}$ must be non-zero. Also, in case $\bar{K}_1 >> \bar{K}_{A0}$, one can verify that $A_M \approx \bar{K}_1/2\gamma_1$ and thus $M \approx \bar{K}_1/2\sqrt{\gamma_1\gamma_2}$. As a consequence, if $\bar{K}_1/\gamma_1$ increases then so must do $\bar{K}_2/\gamma_3$. Finally, $A_m \approx 0$, and $m \approx \sqrt{\bar{K}_{A0}/\gamma_2 A_m}$. As a consequence, the smaller $\bar{K}_{A0}$ becomes, the smaller $\bar{K}_{B0}$ must be (see [15] for more details). Assume that the values of $K_i, k_i, \delta_i, \gamma_i, \delta_A, \delta_B$ have been chosen so that there is a unique equilibrium and we numerically study the occurrence of periodic solutions as the difference in time-scales between protein and m-RNA, ϵ, and the difference in time-scales between activator and repressor, ν, are changed. In particular, we perform bifurcation analysis with ϵ and ν the two bifurcation parameters. These bifurcation results are summarized by Figure 6.8. The reader is referred to [15] for the details of the numerical analysis. In terms of the ϵ and ν parameters, it is thus possible to "over design" the system: if the activator dynamics is sufficiently sped up with respect to the repressor dynamics, the system parameters move across a Hopf bifurcation (Hopf bifurcation was introduced in Chapter 3) and stable oscillations will arise. From a fabrication point of view, the activator dynamics can be sped up by adding suitable degradation tags to the activator protein. The region of

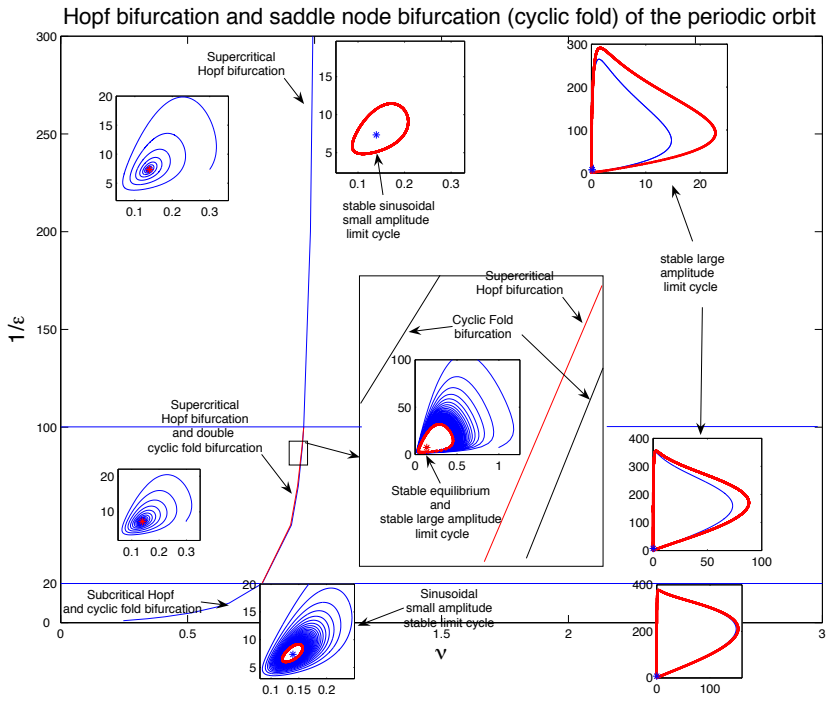

Figure 6.8: Design chart for the relaxation oscillator. One obtains sustained oscillations passed the Hopf bifurcation, for values of ν sufficiently large independently of the difference of time scales between the protein and the mRNA dynamics. We also notice that there are values of ν for which a stable equilibrium point and a stable orbit coexist and values of ν for which two stable orbits coexist. The interval of ν values for which two stable orbits coexist is too small to be able to numerically set ν in such an interval. Thus, this interval is not practically relevant. The values of ν for which a stable equilibrium and a stable periodic orbit coexist is instead relevant. This situation corresponds to the *hard excitation* condition [35] and occurs for realistic values of the separation of time-scales between protein and m-RNA dynamics. Therefore, this simple oscillator motif described by a four-dimensional model can capture the features that lead to the long term suppression of the rhythm by external inputs. *Birhythmicity* [23] is also possible even if practically not relevant due to the numerical difficulty of moving the system to one of the two periodic orbits. For more details, the reader is referred to [15, 12].

the parameter space in which the system exhibits almost sinusoidal damped oscillations is on the left-hand side of the curve corresponding to the Hopf bifurcation. Since the data of [6] exhibits almost sinusoidal damped oscillations, it is possible that the clock is operating in a region of parameter space on the "left" of the curve corresponding to the Hopf bifurcation. If this were the case, increasing the separation of time-scales between the activator and the repressor, ν, may lead to a stable limit cycle.

Another key enabling technology has been the development of *in vivo* measurement techniques that allow to measure the amount of protein produced by a target gene x. For instance, green fluorescent protein (GFP) is a protein with the property that it fluoresces in green when exposed to UV light. It is produced by the jellyfish *Aequoria victoria*, and its gene has been isolated so that it can be used as a reporter gene. The GFP gene is inserted (cloned) into the chromosome, adjacent to or very close to the location of gene x, so both are controlled by the same promoter region. Thus, gene x and GFP are transcribed simultaneously and then translated, so by measuring the intensity of the GFP light emitted one can estimate how much of x is being expressed. Other fluorescent proteins, such as yellow fluorescent protein (YFP) and red fluorescent protein (RFP) are genetic variations of the GFP.

Just as fluorescent proteins can be used as a read out of a circuit, inducers function as external inputs that can be used to probe the system. Inducers function by disabling repressor proteins. Repressor proteins bind to the DNA strand and prevent RNA polymerase from being able to attach to the DNA and synthesize mRNA. Inducers bind to repressor proteins, causing them to change shape and making them unable to bind to DNA. Therefore, they allow transcription to take place.

Inset (Electronic circuits)**.** One of the current directions of the field is to create circuitry with more complex functionalities by assembling simpler circuits, such as those in Figure 6.1. This tendency is consistent with what has been observed in the history of electronics: after the bipolar junction transistor (BJT) was invented in 1947 by William Shockley and co-workers, the transistor era started. A major breakthrough in the transistor era occurred in 1964 with the invention of the first operational amplifier (op amp), which led the way to standardized modular and integrated circuit design. By comparison, synthetic biology may be directing toward a similar development, in which modular and integrated circuit design becomes a reality. This is witnessed by several recent efforts toward formally characterizing interconnection mechanisms between modules, impedance-like effects, and op amp-like devices to counteract impedance problems [26, 49, 48, 17, 47, 52, 51]. ◊

Bibliography

[1] K. J. Åström and R. M. Murray. *Feedback Systems: An Introduction for Scientists and Engineers*. Princeton University Press, 2008. Available at http://www.cds.caltech.edu/~murray/amwiki.

[2] B. Alberts, D. Bray, J. Lewis, M. Raff, K. Roberts, and J. D. Watson. *The Molecular Biology of the Cell*. Garland Science, fifth edition edition, 2008.

[3] U. Alon. *An introduction to systems biology. Design principles of biological circuits*. Chapman-Hall, 2007.

[4] W. Arber and S. Linn. DNA modification and restriction. *Annual Review of Biochemistry*, 38:467–500, 1969.

[5] D. P. Atherton. *Nonlinear Control Engineering*. Van Nostrand, New York, 1975.

[6] M. R. Atkinson, M. A. Savageau, J. T. Meyers, and A. J. Ninfa. Development of genetic circuitry exhibiting toggle switch or oscillatory behavior in *Escherichia coli*. *Cell*, pages 597–607, 2003.

[7] D. W. Austin, M. S. Allen, J. M. McCollum, R. D. Dar, J. R. Wilgus, G. S. Sayler, N. F. Samatova, C. D. Cox, and M. L. Simpson. Gene network shaping of inherent noise spectra. *Nature*, 2076:608–611, 2006.

[8] D. Baker, G. Church, J. Collins, D. Endy, J. Jacobson, J. Keasling, P. Modrich, C. Smolke, and R. Weiss. ENGINEERING LIFE: Building a FAB for biology. *Scientific American*, June 2006.

[9] N Barkai and S Leibler. Robustness in simple biochemical networks. *Nature*, 387(6636):913–7, 1997.

[10] A. Becskei and L. Serrano. Engineering stability in gene networks by autoregulation. *Nature*, 405:590–593, 2000.

[11] F. D. Bushman and M. Ptashne. Activation of transcription by the bacteriophage 434 repressor. *Proc. of the National Academy of Sciences*, pages 9353–9357, 1986.

[12] E. Conrad, A. E. Mayo, A. J. Ninfa, and D. B. Forger. Rate constants rather than biochemical mechanism determine behaviour of genetic clocks. *J. R. Soc. Interface*, 2008.

[13] A. J. Courey. *Mechanisms in Transcriptional Regulation*. Wiley-Blackwell, 2008.

[14] H. de Jong. Modeling and simulation of genetic regulatory systems: A literature review. *Journal of Computational Biology*, 9:67–103, 2002.

[15] D. Del Vecchio. Design and analysis of an activator-repressor clock in *e. coli*. In *Proc. American Control Conference*, 2007.

[16] D. Del Vecchio and H. El-Samad. Repressilators and promotilators: Loop dynamics in gene regulatory networks. In *Proc. American Control Conference*, 2005.

[17] D. Del Vecchio, A. J. Ninfa, and E. D. Sontag. Modular cell biology: Retroactivity and insulation. *Nature/EMBO Molecular Systems Biology*, 4:161, 2008.

[18] M. B. Elowitz and S. Leibler. A synthetic oscillatory network of transcriptional regulators. *Nature*, 403(6767):335–338, 2000.

[19] D. Endy. Foundations for engineering biology. *Nature*, 438:449–452, 2005.

[20] T.S. Gardner, C.R. Cantor, and J.J. Collins. Construction of the genetic toggle switch in *Escherichia Coli*. *Nature*, page 339342, 2000.

[21] D. T. Gillespie. *Markov Processes: An Introduction For Physical Scientists*. Academic Press, 1976.

[22] D. T. Gillespie. A rigorous derivation of the chemical master equation. *Physica A*, 188:404–425, 1992.

[23] A. Goldbeter. *Biochemical Oscillations and Cellular Rhythms: The molecular basis of periodic and chaotic behaviour*. Cambridge University Press, 1996.

[24] D. Graham and D. McRuer. *Analysis of Nonlinear Control Systems*. Wiley, New York, 1961.

[25] J. Greenblatt, J. R. Nodwell, and S. W. Mason. Transcriptional antitermination. *Nature*, 364(6436):401–406, 1993.

[26] L.H. Hartwell, J.J. Hopfield, S. Leibler, and A.W. Murray. From molecular to modular cell biology. *Nature*, 402:47–52, 1999.

[27] S. Hastings, J. Tyson, and D. Webster. Existence of periodic solutions for negative feedback cellular control systems. *J. Differential Equations*, 25:39–64, 1977. .

[28] R. Heinrich, B. G. Neel, and T. A. Rapoport. Mathematical models of protein kinase signal transduction. *Molecular Cell*, 9:957–970, 2002.

[29] C. F. Huang and J. E. Ferrell. Ultrasensitivity in the mitogen-activated proteinkinase cascade. *Proc. Natl. Acad. Sci.*, 93(19):10078–10083, 1996.

[30] B. Ingalls. A frequency domain approach to sensitivity analysis of biochemical networks. *Journal of Physical Chemistry B-Condensed Phase*, 108(3):143–152, 2004.

[31] F. Jacob and J. Monod. Genetic regulatory mechanisms in the synthesis of proteins. *J. Mol. Biol.*, 3:318–56, 1961.

[32] N. G. Van Kampen. *Stochastic Processes in Physics and Chemistry*. Elsevier, 1992.

[33] B. N. Kholodenko, G. C. Brown, and J. B. Hoek. Diffusion control of protein phosphorylation in signal transduction pathways. *Biochemical Journal*, 350:901–907, 2000.

[34] P. Kokotovic, H. K. Khalil, and J. O'Reilly. *Singular Perturbation Methods in Control*. SIAM, 1999.

[35] J.-C. Leloup and A. Goldbeter. A molecular explanation for the long-term supression of circadian rhythms by a single light pulse. *American Journal of Physiology*, 280:1206–1212, 2001.

[36] H. Madhani. *From a to alpha: Yeast as a Model for Cellular Differentiation*. CSHL Press, 2007.

[37] J. Mallet-Paret and H.L. Smith. The Poincaré-Bendixson theorem for monotone cyclic feedback systems. *J. of Dynamics and Differential Equations*., 2:367–421, 1990.

[38] C. J. Morton-Firth, T. S. Shimizu, and D. Bray. A free-energy-based stochastic simulation of the tar receptor complex. *Journal of Molecular Biology*, 286(4):1059–74, 1999.

[39] J. D. Murray. *Mathematical Biology,* Vols. I and II. Springer-Verlag, New York, 3rd edition, 2004.

[40] R. M. Murray. *Optimization-Based Control*. http://www.cds.caltech.edu/~murray/amwiki/OBC, Retrieved 20 December 2009.

[41] National Center for Biotechnology Information. A science primer. Retrieved 20 December 2009, 2004. http://www.ncbi.nlm.nih.gov/About/primer/genetics.html.

[42] National Human Genome Research Institute. Talking glossary of genetic terms. Retrieved 20 December 2009. http://www.genome.gov/glossary.

[43] R. Phillips, J. Kondev, and J. Theriot. *Physical Biology of the Cell*. Garland Science, 2008.

[44] M. Ptashne. *A genetic switch*. Blackwell Science, Inc., 1992.

[45] C. V. Rao, J. R. Kirby, and A. P. Arkin. Design and diversity in bacterial chemotaxis: A comparative study in escherichia coli and bacillus subtilis. *PLoS Biology*, 2(2):239–252, 2004.

[46] N. Rosenfeld, M. B. Elowitz, and U. Alon. Negative autoregulation speeds the response times of transcription networks. *J. Molecular Biology*, 323(5):785–793, 2002.

[47] G. De Rubertis and S. W. Davies. A genetic circuit amplifier: Design and simulation. *IEEE Trans. on Nanobioscience*, 2(4):239–246, 2003.

[48] J. Saez-Rodriguez, A. Kremling, H. Conzelmann, K. Bettenbrock, and E. D. Gilles. Modular analysis of signal transduction networks. *IEEE Control Systems Magazine*, pages 35–52, 2004.

[49] J. Saez-Rodriguez, A. Kremling, and E.D. Gilles. Dissecting the puzzle of life: modularization of signal transduction networks. *Computers and Chemical Engineering*, 29:619–629, 2005.

[50] H. M. Sauro. The computational versatility of proteomic signaling networks. *Current Proteomics*, 1(1):67–81, 2004.

[51] H. M. Sauro and B. Ingalls. MAPK cascades as feedback amplifiers. Technical report, http://arxiv.org/abs/0710.5195, Oct 2007.

[52] H. M. Sauro and B. N. Kholodenko. Quantitative analysis of signaling networks. *Progress in Biophysics & Molecular Biology*, 86:5–43, 2004.

[53] M. A. Savageau. Biochemical systems analysis. i. some mathematical properties of the rate law for the component enzymatic reactions. *J. Theoretical Biology*, 25:365–369, 1969.

[54] D. L. Schilling and C. Belove. *Electronic Circuits: Discrete and Integrated*. McGraw Hill, 1968.

[55] S. S. Shen-Orr, R. Milo, S. Mangan, and U. Alon. Network motifs in the transcriptional regulation network of *Escherichia coli*. *Nat. Genet.*, 31(1):64–68, 2002.

[56] D. Del Vecchio, A. J. Ninfa, and E. D. Sontag. A systems theory with retroactivity: Application to transcriptional modules. In *Proc. American Control Conference*, 2008.

[57] L. Villa-Komaroff, A. Efstratiadis, S. Broome, P. Lomedico, R. Tizard, S. P. Naber, W. L. Chick, and W. Gilbert. A bacterial clone synthesizing proinsulin. *Proc. Natl. Acad. Sci. U.S.A.*, 75(8):372731, 1978.

[58] T.-M. Yi, Y. Huang, M. I. Simon, and J. Doyle. Robust perfect adaptation in bacterial chemotaxis through integral feedback control. *Proc. of the National Academy of Sciences*, 97(9):4649–53, 2000.